JOURNAL OF VIROLOGY, July 2005, p. 8046–8056 Vol. 79, No. 13
0022-538X/05/$08.00+0 doi:10.1128/JVI.79.13.8046–8056.2005

Effects of a Temperature Sensitivity Mutation in the J1R Protein Component of a Complex Required for Vaccinia Virus Assembly

Wen-Ling Chiu,[1] Patricia Szajner,[2] Bernard Moss,[2] and Wen Chang[1]*

Institute of Molecular Biology, Academia Sinica, Nankang, Taipei, Taiwan, Republic of China,[1] and Laboratory of Viral Diseases, NIAID, NIH, Bethesda, Maryland[2]

Received 12 November 2004/Accepted 7 March 2005

Vaccinia virus J1R protein is required for virion morphogenesis (W. L. Chiu and W. Chang, J. Virol. 76:9575–9587, 2002). In this work, we further characterized the J1R protein of wild-type vaccinia virus and compared it with the protein encoded by the temperature-sensitive mutant virus C*ts*45. The mutant C*ts*45 was found to contain a Pro-to-Ser substitution at residue 132 of the J1R open reading frame, which is responsible for a loss-of-function phenotype. The half-life of the J1R-P132S mutant protein was comparable at both 31 and 39°C, indicating that the P132S mutation did not affect the stability of the J1R protein. We also showed that the J1R protein interacts with itself in the virus-infected cells. The N-terminal region of the J1R protein, amino acids (aa) 1 to 77, interacted with the C-terminal region, aa 84 to 153, and the P132 mutation did not abolish this interaction, as determined by two-hybrid analysis. Furthermore, we demonstrated that J1R protein is part of a viral complex containing the A30L, G7L, and F10L proteins in virus-infected cells. In immunofluorescence analyses, wild-type J1R protein colocalized with the A30L, G7L, and F10L proteins in virus-infected cells but the loss-of-function P132 mutant did not. Furthermore, without a functional J1R protein, rapid degradation of A30L and the 15-kDa forms of the G7L and F10L proteins was observed in cells infected with C*ts*45 at 39°C. This study thus demonstrated the importance of the J1R protein in the formation of a viral assembly complex required for morphogenesis.

Vaccinia virus (VV) is the prototypical member of the poxvirus family. Vaccinia virus is a double-stranded DNA virus that replicates in the cytoplasm of infected cells (18). The study of poxviruses is challenging because of the large size of their genomes and their complex structure and composition. In addition, poxviruses produce several distinct infectious particles during their life cycle (9, 17). Virion morphogenesis is highly complex and involves the formation of intermediate viral structures. For example, cytoplasmic viral factories initiate the formation of crescent-shaped membranes that enclose DNA from the virosomes to become immature virions (IV). These nucleoid-containing IV are subsequently converted into the brick-shaped, infectious intracellular mature virions (IMV) (14). IMV become intracellular enveloped virus particles when they are wrapped with membranes derived from Golgi cisternae (28). Intracellular enveloped virus particles are then transported via microtubules to the cell periphery, where they fuse with the plasma membrane and remain as cell-associated virions or are released from the cell as extracellular enveloped viruses (4, 5, 11, 13, 22, 26, 39).

Studies of virion morphogenesis have been facilitated by the use of various inhibitors or by generation of conditional lethal and temperature-sensitive (*ts*) mutant viruses to arrest the virion assembly processes (12, 20, 23, 27). Several viral proteins are known to be essential for IV formation. Viral F10L protein kinase is required for the earliest stage of virion morphogenesis, since no recognizable viral membranes were observed when F10L function was inactivated (32, 37, 41). A14L and A17L proteins are both F10L substrates, and when expression of either protein was repressed, membranes formed but with accumulation of abnormal vesicles in cells (3, 10, 24, 25, 38, 43). Repression of A30L or G7L protein expression resulted in large numbers of crescent-shaped and open circular membranes that were devoid of DNA and granular materials (31, 35). In addition, phosphorylation of A30L was dependent on the F10L kinase, and physical interactions between A30L, G7L, and F10L were demonstrated (33). Finally, we have shown that when vaccinia virus J1R protein expression was repressed, abundant viral membranes were also observed with empty or partially filled IV, indicating that J1R protein also participates in IV formation (6). In this study, we investigate a temperature-sensitive vaccinia virus mutant, C*ts*45, which was originally isolated by Condit and colleagues (7, 8). By comparing the role of wild-type (WT) J1R protein with that of the mutant J1R protein in C*ts*45, we demonstrated the importance of the J1R protein for the integrity of a viral assembly complex.

MATERIALS AND METHODS

Cells, viruses, and yeast strains. BSC40 cells were cultured in Dulbecco's modified Eagle medium (DMEM) supplemented with 10% calf serum, and CV-1 and 293T cells were cultured in DMEM supplemented with 10% fetal bovine serum. WT vaccinia virus (strain WR) was grown in BSC40 cells. A recombinant virus, viJ1R, expressing WT J1R protein under isopropyl-β-D-thiogalactopyranoside (IPTG) regulation, was described previously (6). C*ts*45 virus was obtained from R. Condit (7, 8, 15). *Saccharomyces cerevisiae* strains L40 [*MAT***a** *his3Δ200 trp1-901 leu2-3,112 ade2 LYS*::(*lexAop*) *4-HIS3 URA3*::(*lexAop*) *8-lacZ GAL4*] and AMR70 (*MAT***a** *trp1 leu2 his3 URA3*::*lexA-lacZ*) were used for transformation of the LexA DNA binding domain (BD) and Gal4 activation domain (AD)

* Corresponding author. Mailing address: Institute of Molecular Biology, Academia Sinica, 128, Sec. 2, Academia Road, Nankang, Taipei 11529, Taiwan, Republic of China. Phone: 886-2-2789-9230. Fax: 886-2-2782-6085. E-mail: mbwen@ccvax.sinica.edu.tw.

fusion proteins (40). The yeast strains were maintained at 30°C on YPAD (yeast extract, peptone, and dextrose with 40 μg/ml adenine) plates.

Reagents and Abs. Lipofectamine Plus was purchased from Invitrogen, Inc. Rabbit antibodies (Abs) recognizing J1R, A30L, G7L, F10L, A17L-N, and A17L-C were described previously (3, 6, 31, 32, 35). The monoclonal antibody (MAb) against A45R protein was provided by G. Smith (1). A MAb recognizing the T7 tag was purchased from Novagen Inc.

Immunoblot analyses. Virus-infected cell extracts were fractionated by sodium dodecyl sulfate–15% polyacrylamide gel electrophoresis (SDS–15% PAGE) and transferred to nitrocellulose membranes. Membranes were blocked in 0.2% I-block in phosphate-buffered saline (PBS) plus 0.1% Tween 20 at room temperature for 1 h and incubated with individual primary Abs (anti-J1R [1:1,000], anti-A30L [1:250], anti-G7L [1:1,000], anti-F10L [1:1,000], A17L-N [1:2,000], A17L-C [1:500], and anti-A45R [1:5,000]) at room temperature for 1 h. The membranes were washed and then incubated with secondary antibodies coupled to alkaline phosphatase (1:1,000). The blots were developed by using the substrate CDP-Star (Tropix, Inc.) as described by the manufacturer and by exposure to autoradiogram films.

Radioimmunoprecipitation analysis. BSC40 cells were infected with WT VV or C*ts*45 at a multiplicity of infection (MOI) of 10 PFU per cell for 1 h at 31°C. The infected cells were incubated with DMEM containing 10% calf serum at 31°C or 39°C. At 8 h postinfection (p.i.), the medium was removed and replaced with methionine-free medium for 15 min, and the infected cells were subsequently pulse-labeled with [^{35}S]methionine (50 μCi/ml) for 30 min. After the pulse, cells were immediately washed with PBS, incubated in growth medium with a 100-fold excess of unlabeled methionine (3 mg/ml), and chased for 0, 1, 2, 4, 8, or 16 h. At each time point, cells were washed with cold PBS and lysed with Herman's lysis buffer (1% NP-40–0.5% deoxycholate–0.1 M NaCl–1 mM EDTA–10 mM Tris [pH 8]). Insoluble materials were removed by centrifugation (10,000 × *g*, 10 min, 4°C). Cell lysates were incubated with an anti-J1R Ab (1:100) at 4°C for 2 h, and subsequently 50 ml of protein A-Sepharose (50%) (Amersham Biosciences) was added. The immunoprecipitates were washed five times with lysis buffer, separated on an SDS–15% PAGE gel, and dried for autoradiograms. The films were scanned, and quantification was performed using Fujifilm Image Gauge software.

***trans*-complementation assays. (i) Plasmid construction and site-directed mutagenesis.** The J1R open reading frame (ORF) was generated by PCR amplification from VV strain WR DNA, digested with BamHI, and cloned into pL-Topo, which was derived from the pCRII-TOPO vector (Invitrogen) with an insertion of a synthetic late promoter (5′-AATTGGATCAGCTTTTTTTTTTT TTTTTTTGGCATATAAATAAGA-3′). The resulting plasmid, pL-Topo-J1R, thus expresses J1R protein using a viral synthetic late promoter. Other J1R mutants, such as pL-TopoJ1R-P132D, pL-TopoJ1R-P132G, and pL-TopoJ1R-P132L, were generated from pL-TopoJ1R by site-directed mutagenesis (QuikChange site-directed mutagenesis kit [Stratagene]) using the following and complementary oligonucleotides: P132D (5′-CCTGTTAGATACATAGATGA CCGTCGCAATATCGCATTT-3′), P132G (5′-CCTGTTAGATACATAGAT GGGCGTCGCAATATCGCATTT-3′), and P132L (5′-CCTGTTAGATACAT AGATCTGCGTCGCAATATCGCATTT-3′). The underlined bases represent the mutated codons, and only the sense primers are shown. All the plasmid clones were confirmed by DNA sequencing. We also generated an additional J1R-P132D mutant construct from a T7-tagged WT J1R template DNA (T7-J1R) described before (6) for immunofluorescence analysis by using the same site-directed mutagenesis method described above.

(ii) *trans*-complementation. The *trans*-complementation assays were performed essentially as described elsewhere (42). Confluent 293T cells in 60-mm dishes were infected with viJ1R at an MOI of 5 PFU/cell for 1 h in the absence of IPTG. After infection, cells were washed with PBS, and 2 μg of individual plasmids (pL-TopoJ1R, pL-TopoJ1R-P132D, pL-TopoJ1R-P132G, or pL-TopoJ1R-P132L) was transfected into cells using 10 μl Lipofectamine (Invitrogen). After a 5-h incubation, the mixtures were removed and fresh complete medium was added. Cells were harvested at 24 h p.i. for immunoblot analysis and virus titer determination on BSC40 cells. The T7-tagged WT J1R and T7-tagged P132D mutant constructs were also tested in transient complementation assays as described above, and the results showed that addition of the T7 tag had no effect on J1R protein function.

For marker rescue of C*ts*45, CV-1 cells were transfected with pL-Topo or pL-TopoJ1R as described above. At 4 h after transfection, the cells were infected with C*ts*45 at an MOI of 0.05 PFU/cell and incubated at 39°C for 3 days. The cells were harvested, and the lysates were diluted and used to infect a BSC40 monolayer at 39°C. After 2 days, the monolayer were stained with crystal violet and photographed as described previously (34, 36).

Gel filtration analysis of recombinant T7-J1R protein. The full-length J1R ORF was expressed in pET21a with a T7 tag at the N terminus and a hexahistidine tag at the C terminus (T7-J1R) and purified by nickel column chromatography as described elsewhere (6). Purified T7-J1R protein (50 μg) in PBS was loaded onto a HiPrep 26/60 Sephacryl S-100 High Resolution column (Amersham Pharmacia), and individual fractions of 5 ml volume were collected for a total of 81 fractions using the AKTAprime system (Amersham Biosciences). Samples of three fractions were pooled together and concentrated by precipitation in 10% trichloroacetic acid. These pooled fractions were separated by SDS–12% PAGE and analyzed by immunoblotting with anti-T7 Ab (1:5,000). Markers used for gel filtration analyses included blue dextran (2 MDa), RNase A (15.7 kDa), and ovalbumin (48.6 kDa).

Construction of the recombinant T7-J1R virus. The full-length J1R ORF fused with a T7 tag at the N terminus and hexahistidine sequences at the C terminus (T7-J1R) was described previously (6). The DNA fragment containing the T7-J1R ORF was isolated from the pET21a-J1R plasmid after digestion with NdeI and BlpI and was ligated into a SmaI-digested pSC11 vector so that expression of the T7-J1R ORF is controlled by a viral late p11K promoter. Two micrograms of the resulting plasmid, pSC11-T7-J1R, was transfected into CV-1 cells immediately after infection with viJ1R at an MOI of 5 PFU per cell. These cells were cultured in DMEM with 10% fetal bovine serum in the absence of IPTG, and lysates were harvested at 2 days p.i. Since no plaque is formed by viJ1R without IPTG, only recombinant viruses with the T7-J1R ORF inserted into the *tk* locus of viJ1R could rescue virus growth on BSC40 cells. The recombinant T7-J1R viruses were isolated and purified by three rounds of a plaque purification procedure. The T7-J1R virus expresses only the T7-J1R protein of 21 kDa, with no WT J1R protein detected in immunoblot analyses.

Yeast two-hybrid analysis. (i) Plasmid construction. Each of the primers yJ1R-f (5′-GGATCCGTATGGATCACAACCAGTAT-3′), yJ1R-f31 (5′-GGATCCGTATGTCATTATCTGATATATTG-3′), yJ1Rf58 (5′-GGATCCGTATG GTGGGTCATTGTTATGGA-3′), yJ1Rf84 (5′-GGATCCGTATGCTGTTTA ACAAGGTCCCT-3′), and yJ1Rf109 (5′-GGATCCGTATGAGTTTGATGCG ATTCAAA-3′) was used with yJ1Rr (5′-GGATCCTTAATTATTGTTCACTT T-3′) to amplify various N-terminal deletions of the J1R ORF. The resulting DNA fragments were digested with BamHI and cloned into plasmid pBTM116 or pACT2-AD (Clontech Inc.) (2).

The C-terminal deletions of J1R in pACT2-AD were generated by an ExoIII deletion procedure. Five micrograms of plasmid pACT2-J1R was digested with SacI and EcoRI. The linearized DNA was mixed with ExoIII (500 U) at 29°C for various times, treated with S1 and Klenow fragment, ligated, and transformed into *Escherichia coli*. These C-terminal deletion fragments of the J1R ORF were subsequently excised from pACT2-AD with HindIII and ligated into pBTM116. Restriction enzyme digestion and DNA sequencing were performed to confirm the orientations of all DNA constructs.

(ii) Yeast transformation and two-hybrid analyses. Transformation procedures were performed as described previously (40). To prepare competent yeast, several yeast colonies were incubated in 10 ml YPAD medium at 30°C overnight. A stationary-phase yeast culture was diluted into 50 ml YPAD medium and grown for 4 h at 30°C. Yeast cells were collected by centrifugation at 2,500 rpm for 5 min at room temperature, washed once with H_2O, and suspended in 2 ml of 0.5× Tris-EDTA (TE)–100 mM lithium acetate (LiAc). For small-scale transformation, 1 μg of DNA and 10 μl of herring sperm carrier DNA (Clontech) were mixed with 100 μl of competent yeast cells. After addition of 700 μl of a polyethylene glycol (PEG)-LiAc solution (100 mM LiAc–1× TE–40% PEG 3350), the mixture was incubated first at 30°C for 30 min and then at 42°C for 30 min and centrifuged. The pellet was washed once with 1× TE and resuspended in 1× TE for plating on SD/-Leu or SD/-Trp (minimal synthetic dropout medium lacking leucine or tryptophan, respectively) plates. Colonies were isolated in 3 days.

To detect interactions between proteins, the transformants in yeast L40 and AMR70 were mated on YPAD plates for 3 days at 30°C and transferred to SD/-Leu/-Trp plates for another 3 days. The resulting Leu^+ Trp^+ colonies were further plated on SD/-Leu/-Trp/-His plates containing 2.5 to 20 mM 3-amino-1,2,4-triazole (3-AT) to select for growth of Leu^+ Trp^+ His^+ colonies in 3 to 7 days. AD and BD cloning vectors alone did not grow on SD/-Leu/-Trp/-His plates containing 2.5 to 20 mM 3-AT.

Electron and confocal microscopy. For electron microscopy (EM), BSC40 cells were seeded on round coverslips and infected with viJ1R or C*ts*45 at an MOI of 20 PFU per cell. These cells were directly fixed on coverslips at 24 h p.i. in 2.5% glutaraldehyde in 0.1 M PBS (pH 7.0) at room temperature for 1 h and rinsed in three 15-min changes of 0.1 M sodium phosphate buffer (pH 7.0). Cells were treated with 1% OsO_4 in 0.1 M sodium phosphate (pH 7.0) at room temperature for 60 min and washed three times in 0.1 M sodium phosphate (pH 7.0). Cells

were dehydrated using an ethanol series from 30% to 100% ethanol, and Spurr's resin was used for infiltration and embedding as described elsewhere (29). After embedding, cells were separated from coverslips and thin sectioned with an Ultracut Eultramicrotome. Thin sections of 90 nm were stained with uranyl acetate and lead citrate and analyzed under a Zeiss 902 transmission electron microscope (21).

For confocal microscopy, BSC40 cells (7×10^4) were seeded on round glass slides in 12-well plates overnight and infected with viJ1R at an MOI of 10 PFU/cell at 37°C for 1 h. The infected cells were subsequently transfected with 0.4 μg of T7-tagged forms of WT J1R or P132D plasmid, incubated in medium without IPTG for 24 h, and fixed in freshly prepared 4% paraformaldehyde at 4°C for 20 min. Cells were rinsed in PBS five times and permeabilized in 1% Triton X-100–PBS for 5 min and in 0.5% Tween 20–0.5% bovine serum albumin–PBS for 15 min at room temperature. The cells were blocked with 1% bovine serum albumin–PBS for 1 h, incubated with Abs against the T7 tag (1:2,000) and A30L (1:250) for 1 h, and then incubated with an Alexa Fluor 488 $F(ab')_2$ fragment of goat anti-mouse immunoglobulin G (heavy plus light chains) (1:1,000) (Molecular Probes) and Cy5-conjugated AffiniPure goat anti-rabbit immunoglobulin G (heavy plus light chains) (1:1,000) (Jackson ImmunoResearch Laboratories, Inc.) for 1 h. The samples were washed with PBS, mounted in Vectashield (Vector Laboratories, Inc.), and analyzed using a Zeiss LSM 510 confocal microscope.

Coimmunoprecipitation. Coimmunoprecipitation experiments of WT J1R with A30L, G7L, and F10L proteins were performed as described previously (33). In brief, BSC-1 cells were infected with vT7LacOI or vA30iHA virus in the presence of 50 μM IPTG. At 24 h p.i., cell extracts were prepared and incubated with an anti-hemagglutinin (anti-HA) antibody conjugated to agarose beads. The immunoprecipitated products were analyzed by electrophoresis on an SDS–10 to 20% Tricine gel, followed by immunoblotting using an anti-G7L Ab, an anti-J1R Ab, or an anti-HA MAb conjugated to horseradish peroxidase (HRP). Alternatively, BSC-1 cells were infected with wild-type VV (WR) or vWT-F10V5 (WR containing a V5-tagged copy of the F10 protein), and cell extracts were prepared at 24 h p.i. for immunoprecipitation with an anti-V5 MAb conjugated to agarose beads and were analyzed with either an anti-V5 Ab conjugated to HRP, an anti-G7L Ab, an anti-J1R Ab, or an anti-A30L Ab.

For the J1R self-interaction experiment, BSC40 cells were coinfected with T7-J1R virus and viJ1R at an MOI of 5 PFU per cell and incubated in medium containing 50 μM IPTG. Cells were harvested at 24 h p.i. for immunoprecipitation using an anti-T7 MAb (1:1,000), followed by protein A/G beads as described above. The immunoprecipitated products were separated on an SDS–12% PAGE gel, and the proteins were detected by anti-T7 and anti-J1R Abs as described above.

RESULTS

The J1R open reading frame of C*ts*45 contains a predicted proline-to-serine mutation at residue 132. A *ts* mutant, C*ts*45, with a genetic defect in the J1R gene defined by complementation analysis, was obtained from R. Condit (15). The *ts* mutant formed plaques at 31°C and, when the J1R gene was transfected into cells, formed plaques at 39°C (Fig. 1A), consistent with the previous report (15). We then infected BSC40 cells with C*ts*45 virus at a permissive (31°C) or nonpermissive (39°C) temperature and compared virion morphogenesis with that of the IPTG-inducible mutant virus viJ1R by EM (Fig. 1B). At 31°C, normal morphology of IMV was observed in cells infected with C*ts*45 and viJ1R in the presence of IPTG (Fig. 1B, top panels). At 39°C, a blockage of virion morphogenesis was observed, with accumulation of single- and multiple-layer viral membrane structures separated from large masses of dense granular material, similar to that observed for viJ1R in the absence of IPTG (Fig. 1B, bottom panels). Furthermore, viral p4a/4b core protein processing, as monitored by a pulse-chase experiment with [^{35}S]methionine, was severely blocked, as for viJ1R in the absence of IPTG (Fig. 1C). DNA sequencing analysis of the J1R ORF in C*ts*45 identified a single C-to-T mutation, resulting in a Pro-to-Ser substitution at amino acid 132 (Fig. 1D). Proline at residue 132 is conserved in all J1R orthologues in poxviruses, implying an important role for J1R functions.

P132S mutation does not affect J1R protein stability in C*ts*45-infected cells. The phenotype of a *ts* mutant could result from misfolding of the mutant protein at the nonpermissive temperature, leading either to protein instability or to a loss of function. We thus monitored the amount of J1R protein expressed in wild-type virus- or C*ts*45 virus-infected cells at 31 and 39°C (Fig. 2A). J1R protein is a late gene product and was detected in late-phase cell lysates harvested from 8 to 24 h p.i. Both WT J1R and mutant P132S proteins were accumulated in virus-infected cells, although they were more abundant at 31°C than at 39°C, suggesting that P132S mutation does not preferentially affect J1R protein stability. To get a more precise measurement of J1R protein stability, we performed pulse-chase experiments to compare the stabilities of WT J1R and mutant P132S proteins. BSC40 cells were infected with WT VV or C*ts*45 at 31 and 39°C, pulse-labeled with [^{35}S]methionine for 30 min at 8 h p.i., and chased for various times. J1R protein was immunoprecipitated with an anti-J1R Ab and analyzed by SDS–15% PAGE (Fig. 2B). Quantification of the intensity of J1R protein revealed that the half-lives of WT J1R and mutant P132S proteins were around 4.5 and 3.5 h at 31°C, respectively, and little difference was observed when the temperature was shifted to 39°C (Fig. 2C). Although the stability of P132S mutant protein was slightly reduced relative to the WT J1R protein, the difference was not temperature dependent. We have also harvested the cells and performed denatured immunoprecipitation, and the results also revealed that the half-life of the P132S mutant was around 3 h at both temperatures (data not shown). Thus, the loss of function of P132S mutant protein at 39°C is not due to a lower J1R protein level in cells. We thus concluded that P132S mutation is likely to cause a malfunction of J1R protein.

P132 is located within the C-terminal region of J1R that interacts with the N-terminal region in yeast two-hybrid analysis. Previously, the full-length J1R protein was shown to self-interact by yeast two-hybrid analysis (16). When we expressed a full-length T7-tagged J1R soluble protein (T7-J1R) in *E. coli* (Fig. 3A), we employed Sephacryl S-100 gel filtration analysis to determine the oligomeric state of the recombinant T7-J1R protein. Soluble T7-J1R protein did not elute as a monomer of 21 kDa; instead, it behaved like an oligomer, with a molecular weight consistent with a trimer, in fractions preceding the 48.6-kDa marker protein (Fig. 3B). To provide direct evidence for J1R protein self-interaction in virus-infected cells, we generated a recombinant T7-J1R vaccinia virus expressing the above T7-J1R protein from a viral late promoter as described in Materials and Methods. BSC40 cells were coinfected with viJ1R (in the presence of IPTG) and T7-J1R viruses, and the lysates were harvested at 24 h p.i. for coimmunoprecipitation analyses (Fig. 3C). An anti-T7 MAb immunoprecipitated T7-J1R protein from T7-J1R virus-infected cells. The anti-T7 MAb did not immunoprecipitate WT J1R protein from viJ1R-infected cells (data not shown). Furthermore, in BSC40 cells that were coinfected with both viruses, immunoprecipitation of T7-J1R protein with the anti-T7 MAb also brought down WT J1R protein, demonstrating that T7-J1R protein interacts with WT J1R protein in virus-infected cells. We therefore con-

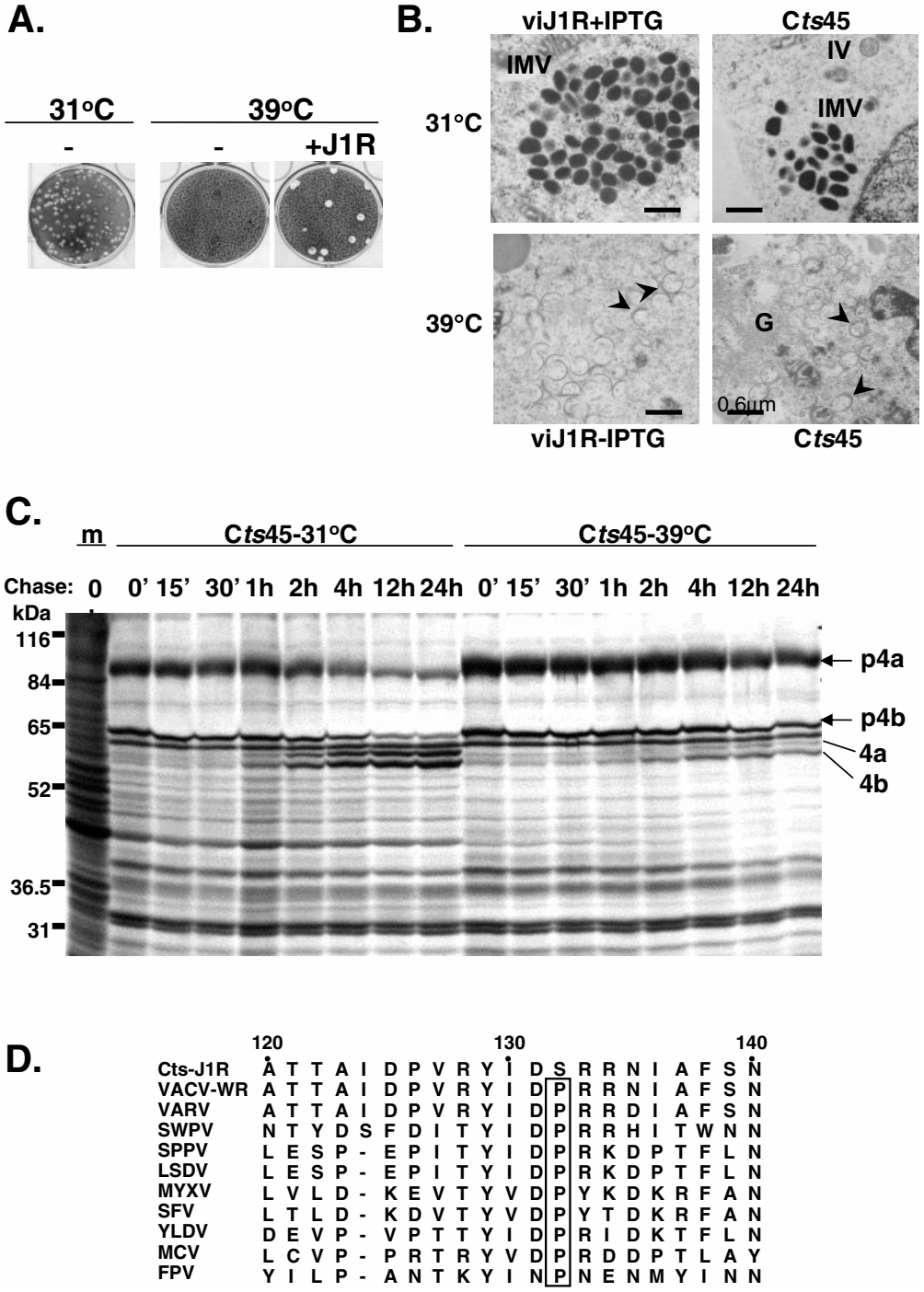

FIG. 1. (A) Marker rescue of C*ts*45. CV-1 cells were transfected with either the plasmid vector (−) or the plasmid containing the WT J1R ORF (+J1R) and infected with C*ts*45 as described in Materials and Methods (34, 36). These cells, incubated at 31 or 39°C, were fixed, stained with crystal violet, and photographed. (B) Electron microscopy of BSC40 cells infected with viJ1R or C*ts*45 at 31 or 39°C. BSC40 cells were infected with viJ1R, with or without 50 μM IPTG, or with C*ts*45. The cells were cultured at 31°C or 39°C for 24 h and processed for EM as described elsewhere (6). G, granular materials. Arrowheads represent double-layer viral membranes that are accumulated at 39°C. (C) Pulse-chase experiment for precursor p4a/p4b protein processing. BSC40 cells were either mock infected (m) or infected with C*ts*45 at an MOI of 10 PFU per cell and incubated at 31°C or 39°C. At 8 h p.i., the cells were pulse-labeled with [^{35}S]methionine for 30 min and chased with normal medium for 0 min, 15 min, 30 min, 1 h, 2 h, 4 h, 12 h, or 24 h. Proteins were denatured and analyzed by SDS–12% PAGE followed by autoradiography. The mobilities of p4a and p4b and their mature processed forms 4a and 4b are shown on the right. (D) Amino acid mutation of J1R protein in C*ts*45. DNA sequences of the J1R gene in C*ts*45 revealed a single nucleotide change from C to T, resulting in a P-to-S change at residue 132. P132 is boxed, indicating that it is invariable in all the J1R orthologues. The alignment shown here contains J1R protein sequences only from amino acid residue120 to 140. VACV-WR, vaccinia virus strain WR; VARV, variola virus (INDIA-1967/isolate IND3); SWPV, swinepox virus; SPPV, sheep poxvirus; LSDV, lumpy skin disease virus; MYXV, myxoma virus; SFV, Shope fibroma virus; YLDV, Yaba-like disease virus; MCV, molluscum contagiosum virus subtype 1; FPV, fowlpox virus.

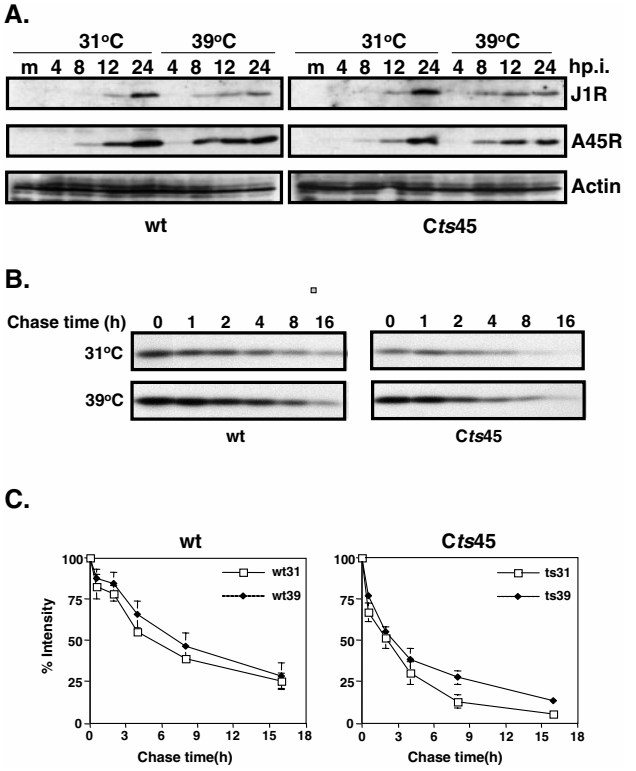

FIG. 2. Stability of J1R protein in cells infected with the WT or C*ts*45 virus under permissive and nonpermissive conditions. (A) Expression of J1R protein in cells infected with WT VV or C*ts*45 at 31 or 39°C. BSC40 cells were either mock infected (m) or infected with WT VV or C*ts*45, incubated at 31 or 39°C, and harvested at different times as indicated for immunoblot analyses with an anti-J1R, anti-A45R, or anti-actin Ab. (B) Pulse-chase experiments with J1R protein. BSC40 cells were infected with WT VV or C*ts*45 at an MOI of 10 PFU per cell and incubated at 31°C or 39°C. At 8 h p.i., the cells were pulse-labeled with [^{35}S]methionine (50 μCi/ml) for 30 min and then chased with normal medium for 0, 1, 2, 4, 8, or 16 h. Cell lysates were immunoprecipitated with anti-J1R (1:100), analyzed by SDS–15% PAGE, and autoradiographed. (C) Quantification of J1R protein from scanning of autoradiograms shown in panel B. The *y* axis represents the percentage of J1R protein present during the chase period, calculated as (intensity of J1R with chase)/(intensity of J1R without chase) × 100%.

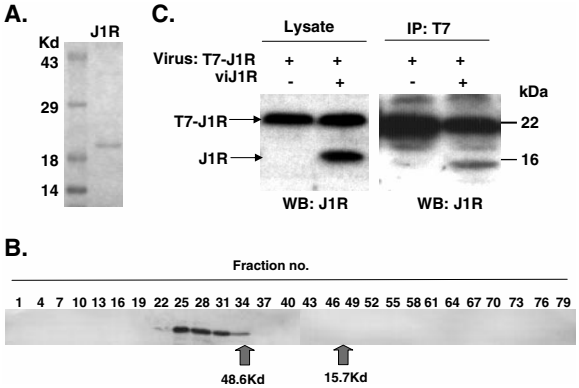

FIG. 3. Self-interaction of J1R protein. (A) Recombinant T7-J1R protein was expressed and purified from *E. coli* as described in Materials and Methods. (B) Gel filtration analysis of the recombinant J1R protein. Purified J1R (50 μg) in PBS was loaded onto a HiPrep 26/60 Sephacryl S-100 High Resolution column (Amersham Pharmacia), and individual fractions were collected. Every three fractions were pooled, separated on an SDS–12% PAGE gel, and analyzed by immunoblotting with an anti-T7 Ab (1:5,000). Markers used for gel filtration analyses included blue dextran (2 MDa), RNase A (15.7 kDa), and ovalbumin (48.6 kDa). (C) Coimmunoprecipitation of WT J1R protein with T7-J1R protein in virus-infected cells. BSC40 cells were coinfected with T7-J1R virus and viJ1R at an MOI of 5 PFU per cell and cultured in a medium containing IPTG. Cell lysates were prepared at 24 h p.i. for immunoprecipitation (IP) using an anti-T7 MAb (1:1,000). The immunoprecipitated products were separated on an SDS–12% PAGE gel, and both T7-J1R (21 kDa) and WT J1R protein (16 kDa) were detected by an anti-J1R Ab (1:1,000). WB, Western blotting.

cluded that J1R protein self-interacts not only in yeast two-hybrid analyses but also in virus-infected cells.

We next wanted to map the self-interacting domains of J1R protein in order to determine whether the P132 mutation would affect J1R's self-interaction capability. Various truncations from the N and C termini of the J1R ORF were fused with the yeast AD or the BD and tested for specific interactions based on His$^+$ colony growth under the 2.5 mM 3-AT condition (Fig. 4) (16). Stronger protein-protein interaction resulted in colony growth even at higher concentrations of 3-AT, i.e., in the 5 to 20 mM range. J1R-AD constructs with the C-terminal sequences up to residue 78 deleted remained competent for binding to the full-length J1R-BD protein, whereas a further deletion up to residue 41 abolished such interaction (Table 1). This result therefore revealed that the minimal self-interaction region at the N terminus is residues 1 to 77.

We then generated several N-terminal deletions from the full-length J1R-BD for mating with the minimal J1R(1-77)-AD construct. The results in Table 2 showed that three N-terminal deletion clones—J1R(31-153)-BD, J1R(58-153)-BD, and J1R(84-153)-BD—bound to the J1R(1-77)-AD fusion protein

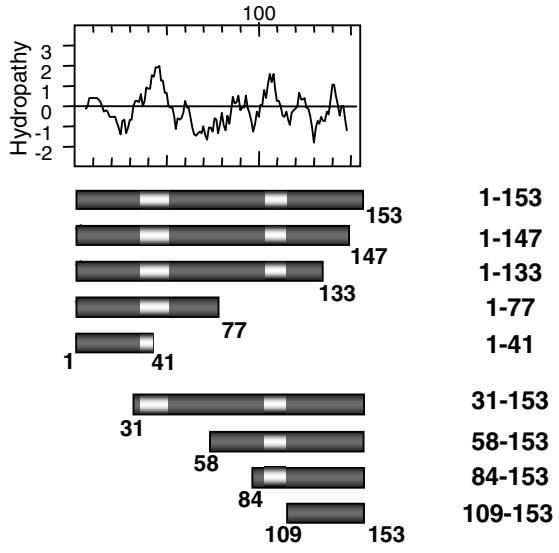

FIG. 4. Deletion constructs of J1R protein used in the yeast two-hybrid analyses. A hydrophathy plot of J1R protein is shown at the top, and all the N- or C-terminal J1R deletion constructs are shown below. The white boxes indicate the two hydrophobic regions previously described (6). Inclusive positions of amino acids present in each J1R deletion construct are given on the right.

TABLE 1. Interaction of full-length BD-J1R (amino acids 1 to 153) with various AD-J1R C-terminal deletion constructs in yeast two-hybrid interaction assays

AD fusion (amino acids)	Interaction with BD-J1R(1–153) at the following 3-AT concn (mM)[a]:			
	2.5	5	10	20
J1R(1-153)	+	+	+	+
J1R(1-147)	+	+	+	+
J1R(1-133)	+	+	+	+
J1R(1-77)	+	+	+	−
J1R(1-41)	−	−	−	−

[a] AD and BD vectors show no background interaction at these concentrations.

but J1R(109-153)-BD did not. These results showed that the minimal C-terminal interacting region is residues 84 to 153. Finally, when we switched the N-terminal J1R(1-77) construct into the BD vector and the C-terminal J1R(84-153) construct into an AD vector, we still obtained an interaction, indicating that fusion of J1R to either the BD or the AD fusion domain did not affect such an interaction (data not shown). Besides, J1R(1-77)-AD did not bind to the homologous region in the BD construct, i.e., J1R(1-77)-BD, nor does J1R(84-153)-AD bind to itself. Taken together, our results revealed that the N-terminal region of the J1R protein interacts with its own C terminus. It is worth noting that residue P132 is located within the C-terminal self-interacting domain.

A non-*ts* mutation of P132 does not abolish J1R self-interaction. Since WT J1R protein could self-interact in yeast two-hybrid analyses, we wanted to test whether the P132S mutation affects the self-interaction activity in any way. However, $J1R^{P132S}$ in *Cts*45 became inactive only at 39°C, a temperature unsuited to performing yeast two-hybrid analysis. We therefore performed site-directed mutagenesis to screen for a P132 mutant allele that had lost J1R function independently of temperature effects, i.e., a lethal mutation at both 31 and 39°C. In vitro mutagenesis was performed to change P132 into G, L, or D, with a lesser degree of conservation toward the latter amino acids. Plasmids containing these mutant J1R alleles were then transfected into 293T cells for transient complementation assays using cells infected with viJ1R in the absence of IPTG in order to determine which of these mutant proteins had lost the ability to complement the J1R deficiency of viJ1R at 37°C (Fig. 5). All the plasmids expressed comparable levels of J1R protein in immunoblots (Fig. 5A). Expression of the WT J1R plasmid produced a 640-fold increase in the virus titer compared to that of the control vector (Fig. 5B). Similarly, the P132G and P132L mutants also rescued the growth of viJ1R, indicating that these two mutations did not inactivate J1R function. In contrast, the P132D mutant was unable to complement the growth of J1R-deficient virus at 37°C, an effect similar to the loss of function by the P132S mutant in *Cts*45-infected cells at 39°C. More importantly, the P132D mutant remained inactive at 31°C, allowing us to investigate mutant J1R self-interaction in yeast two-hybrid analysis (Fig. 5B).

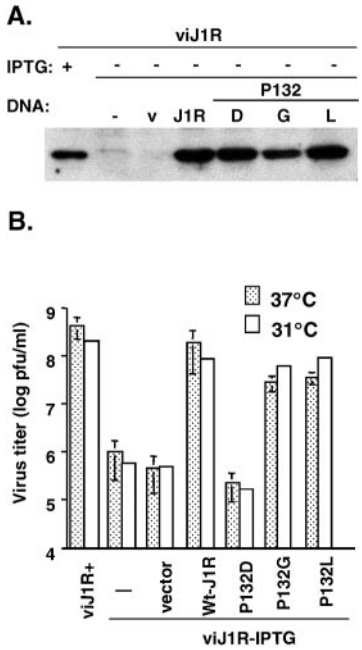

FIG. 5. Transient complementation of viJ1R with various P132 mutant J1R proteins. (A) Immunoblot analysis of J1R mutant proteins. 293T cells at 31 or 37°C were infected with viJ1R in the presence (+) or absence (−) of IPTG and transfected with either vector DNA (v), WT J1R (J1R), or a P132 mutant J1R construct (P132D, P132G, or P132L). Extracts were harvested at 24 h p.i., resolved by SDS–15% PAGE, and analyzed by immunoblotting using an anti-J1R Ab (1:1,000). Only the J1R protein expression at 37°C is shown here. (B) Virus titer determinations by transient complementation assays. Aliquots of cell extracts harvested from 293T cells as described for panel A were used for plaque assays on BSC40 cells at either 31 or 37°C in the presence of 50 μM IPTG as described in Materials and Methods.

TABLE 2. Interaction of AD-J1R (amino acids 1 to 77) with various BD-J1R deletion constructs in yeast two-hybrid interaction assays

BD fusion (amino acids)	Interaction with AD-J1R(1–77) at the following 3-AT concn (mM)[a]:			
	2.5	5	10	20
J1R(31-153)	+	+	+	−
J1R(58-153)	+	+	+	+
J1R(84-153)	+	+	+	+
J1R(109-153)	−	−	−	−
J1R(1-77)	−	−	−	−
31-153(P132D)	+	+	−	−
58-153(P132D)	+	+	+	+
84-153(P132D)	+	+	+	+

[a] AD and BD vectors show no background interaction at these concentrations.

The P132D mutant J1R was fused with the BD of yeast two-hybrid plasmids and tested for interaction with the WT J1R(1-77)-AD construct in yeast two-hybrid analysis as shown in Table 2. All the C-terminal deletion constructs containing the P132D mutation remained interactive with the N-terminal (residues 1 to 77) region of J1R protein, showing that replacement of Pro with Asp does not affect J1R self-interaction. Both the binding of BD-J1R(31-153) and that of BD-31-153(P132D) to AD-J1R(1-77) were slightly weaker than that of other constructs, i.e., negative at 10 to 20 mM 3-AT, indicating that the internal sequences between residues 31 and 57 may have a minor interference effect. Since the difference was minor and not specific to the P132D mutant construct, we concluded that

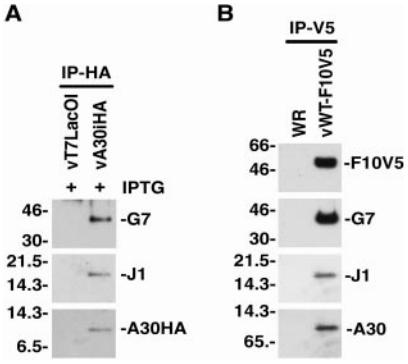

FIG. 6. Coimmunoprecipitation of J1R protein with F10L, G7L, and A30L proteins from VV-infected cells. (A) Coimmunoprecipitation of J1R protein with an anti-HA Ab recognizing A30L protein in virus-infected cells. BSC-1 cells were infected with vT7LacOI or vA30iHA virus in the presence (+) of 50 μM IPTG. At 24 h p.i., cell extracts were prepared and incubated with the anti-HA antibody conjugated to agarose beads. The immunoprecipitated (IP) products were analyzed by electrophoresis on an SDS–10 to 20% Tricine gel, followed by immunoblotting using an anti-G7L Ab, an anti-J1R Ab, or an anti-HA MAb conjugated to HRP. (B) Coimmunoprecipitation of J1R protein with an anti-V5 Ab recognizing F10L in virus-infected cells. BSC-1 cells were infected with wild-type VV (WR) or vWT-F10V5 (WR containing a V5-tagged copy of the F10 protein) as described previously (33). At 24 h p.i., cell extracts were prepared for immunoprecipitation with the anti-V5 MAb conjugated to agarose beads and were analyzed as described for panel A by using either an anti-V5 Ab conjugated to HRP or an anti-G7L, anti-J1R, or anti-A30L Ab, as indicated. Numbers on the left correspond to molecular masses (in kilodaltons) of the marker proteins.

inactivation of J1R function via mutation of P132 does not significantly affect the ability of J1R self-interaction.

WT J1R protein associates with the A30L-containing viral protein complex in VV-infected cells, but the P132D mutant protein has altered distribution. We next determined if the P132S (or P132D) mutation could interfere with J1R's ability to interact with other viral proteins. To test this hypothesis, we first needed to identify the viral proteins to which WT J1R protein binds during IV formation. The A30L protein was a good candidate, since the phenotypes of A30L (35) and J1R (6) inducible mutants are very similar under nonpermissive conditions. It is also known that A30L binds to other viral proteins, including G7L and F10L, during morphogenesis (31, 32, 35), and the above similar genetic mutant phenotype implied that J1R protein might also be a component of A30L-containing complexes. We thus performed coimmunoprecipitation analyses using an anti-HA MAb recognizing HA-tagged A30L protein from cells infected with vA30iHA in the presence of IPTG for 24 h (Fig. 6A). Coimmunoprecipitations were also performed with an anti-V5 MAb to immunoprecipitate F10 kinase from cells infected with the recombinant virus vWT-F10V5 at 24 h p.i. (Fig. 6B). Western blot analyses of these two immunoprecipitates confirmed the presence of A30L, F10L, and G7L proteins in these complexes, as previously shown (33). Most importantly, WT J1R protein was also detected in both immunoprecipitates, indicating that it is present in the same complex containing F10L, G7, and A30 proteins in the virus-infected cells, although their association could be mediated through other proteins within the complex.

Next, we performed immunofluorescence analyses to determine whether J1R and its above-mentioned associated proteins colocalize in virus-infected cells at 24 h p.i. Because our anti-J1R Abs were not suitable for immunostaining WT J1R protein, we used a T7-tagged J1R protein that was transiently expressed in cells infected with viJ1R in the absence of IPTG. The T7 tag did not affect J1R protein function, as determined by complementation (data not shown). The anti-T7 tag Ab detected J1R protein distribution throughout the nucleus and cytoplasmic areas, with more-concentrated staining in the perinuclear virosome regions (Fig. 7A, C, and E). A30L protein had a more localized staining than J1R protein and colocalized with J1R protein in virosomes in virus-infected cells (Fig. 7A). G7L protein also showed colocalization with J1R protein at the perinucelar virosome region (Fig. 7C). The more diffuse staining of J1R protein may have been caused by overexpression. To our surprise, F10L protein staining in virus-infected cells appeared more dispersed than A30L and G7L protein staining. The perinuclear virosome region contained only strong J1R protein staining, with little F10L protein. Instead, colocalization of J1R and F10L staining was seen at more distal and scattered regions in cells (Fig. 7E). At an earlier time point, i.e., 8 h p.i., a more localized virosomal staining of both F10L and J1R proteins was observed (Fig. 7E inset), suggesting that distribution of F10L protein in cells is very dynamic and that, besides the J1R, A30L, and G7L proteins, F10L protein may interact with other proteins in cells. In agreement with our interpretation, a recent study of F10L by Punjabi and Traktman also suggested that F10L plays essential roles at multiple stages in virion morphogenesis, unlike the J1R, A30L, and G7L proteins (19).

Finally, we examined whether the P132 mutation of J1R protein caused aberrant intracellular localization of J1R protein in virus-infected cells (Fig. 7B, D, and F). The P132D mutant was transiently expressed in cells infected with J1R-deficient virus, and cells were stained in order to locate the mutant protein in the infected cells. The P132D mutant J1R protein was detected as a dispersed nuclear and cytoplasmic staining, with no particular concentration at the nuclear periphery of cells. In the same cell, A30L staining aggregated in a speckled pattern surrounding the nuclear periphery (Fig. 7B). Most importantly, no significant colocalization of these two proteins was observed. Similarly, staining of G7L and F10L proteins in cells expressing P132D mutant J1R protein also appeared speckle-like, with no obvious colocalization (Fig. 7D and F). We therefore concluded from the immunofluorescence analyses that the P132D mutation disrupted the ability of J1R protein to associate with A30L, G7L, and F10L proteins in the infected cells.

The P132 mutation and elevated temperature lead to degradation of A30L, F10L, and the 15-kDa form of G7L protein in C*ts*45-infected cells. We now wanted to confirm whether P132S mutant protein behaved similarly to the P132D mutant J1R protein in cells infected with C*ts*45 virus at 39°C. BSC40 cells were infected with C*ts*45 and fixed at 24 h p.i. for immunofluorescence staining with J1R and A30L proteins. However, as many as 70% of the *Cts*45-infected cells contained no A30L protein detectable by immunofluorescence staining at 39°C (data not shown). This was somewhat unexpected, because A30L protein was detected in cells infected with viJ1R in

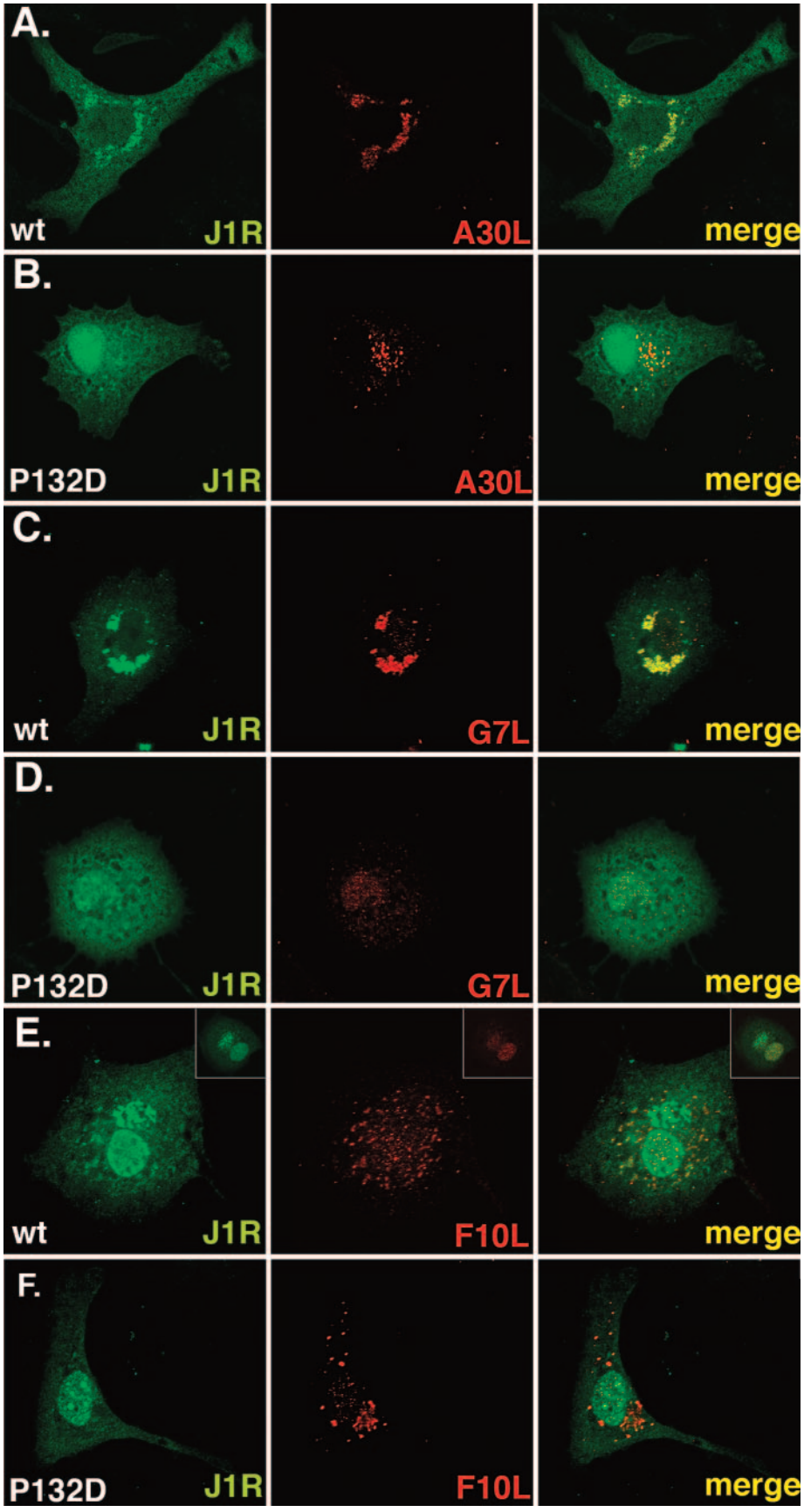

FIG. 7. Intracellular localization of J1R, A30L, G7L, and F10L proteins in virus-infected cells by confocal microscopy. BSC40 cells were infected with viJ1R and transfected with either T7-tagged WT J1R (A, C, and E) or P132D mutant (B, D, and F) constructs. Cells were cultured in medium without IPTG for 24 h, fixed, permeabilized, and stained for viral proteins as shown in each panel. Insets in panel E show immunofluorescence of J1R and F10L proteins in virus-infected cells harvested at 8 h p.i.

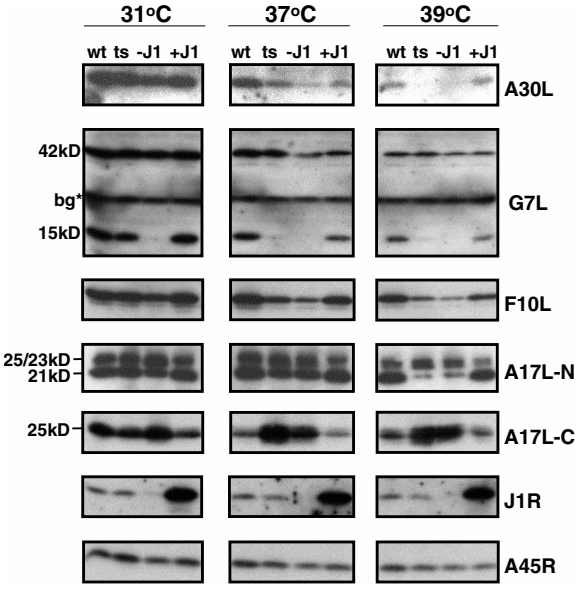

FIG. 8. Immunoblots of J1R-associated viral proteins in virus-infected cells at different temperatures. BSC40 cells were infected with WT VV (wt), *Cts*45 (ts), or viJ1R in the presence (+J1) or absence (−J1) of 50 μM IPTG at an MOI of 5 PFU per cell and were cultured at 31, 37, or 39°C. At 24 h p.i., cells were harvested for immunoblot analysis with an anti-A30L, anti-G7L, anti-F10L, anti-A17L-N or -C, anti-J1R,or anti-A45R Ab. The anti-G7L Ab recognized the 42-kDa precursor protein and the 15-kDa C-terminal cleavage product, as described previously (31). A background band (bg) that was already present in mock-infected cell lysates was marked with an asterisk.

the absence of IPTG, although at a slightly reduced level. Further experiments were carried out to determine whether the instability of A30L protein was due to temperature per se or to enhanced lability in the absence of J1R protein. To demonstrate that the different levels of A30L protein in cells infected with *Cts*45 and viJ1R were results of temperature, we incubated these infected cells at 31, 37, or 39°C (Fig. 8). Without J1R protein, A30L protein levels were slightly reduced in cells infected with viJ1R at 31°C (Fig. 8A, top left panel). When the temperature was raised to 37 and 39°C, A30L protein became undetectable in these cells. It thus appeared that, without a functional J1R protein, degradation of A30L protein occurred in a temperature-dependent manner.

We also investigated whether the stability of G7L and F10L proteins is also affected by inactivation of J1R protein in these virus-infected cells (Fig. 8). When we monitored the levels of G7L protein on immunoblots, two bands of 42 kDa and 15 kDa were identified (Fig. 8, second row). It was previously reported that G7L encodes a full-length protein of 42 kDa which, after proteolytic cleavage at residue 238, produces a 15-kDa C-terminal cleavage product during virion morphogenesis (31). The level of the 42-kDa form of the G7L protein was not affected by J1R protein expression, whereas the 15-kDa cleavage product was detected only in cells expressing a functional J1R protein, regardless of the incubation temperature. The lack of the 15-kDa form of G7L protein in these J1R$^-$ cells did not result in any increased accumulation of the 42-kDa precursor form, implying to us that the degradation occurred after the proteolytic cleavage. Finally, the level of F10L protein was also reduced in viJ1R-infected cells without IPTG and in *Cts*45-infected cells at the elevated temperature, indicating that the stability of F10L protein was also affected in a temperature-dependent manner (Fig. 8, third row). In agreement with this result, the F10L-dependent processing of A17L protein was also reduced upon inactivation of J1R, with accumulation of the 25-kDa A17L precursor protein recognized by an anti-A17L-N Ab that recognized all forms of A17L protein (Fig. 8, fourth row) and an anti-A17L-C Ab that recognized only the precursor form (Fig. 8, fifth row) (3). In summary, J1R protein is important for the stability of A30L, F10L, and the15-kDa form of G7L protein. The mechanism by which J1R protein regulates the stability of these proteins is unknown but appears rather specific, since the stability of the A45R protein, another J1R-binding protein but one that is dispensable for virion morphogenesis, was not reduced at any of the three temperatures (Fig. 8, bottom row). We therefore concluded that the association of J1R protein with the A30L, G7L, and F10L proteins is a critical step in IV formation. When J1R protein was not incorporated into the viral assembly complex, the resulting virion assembly complex was not properly folded, leading to degradation of the component proteins of the complex.

DISCUSSION

Our previous work showed that J1R protein is required for IV morphogenesis (6). In this study, we took two approaches to dissect the function of J1R protein further. First, we obtained the *Cts*45 mutant from the Condit collection in order to understand the structure and function of J1R protein (15). In addition, we searched for other vaccinia virus mutants with a phenotype similar to that of the J1R-deficient virus with the expectation that these mutants may reveal other viral proteins acting in concert with J1R protein for IV formation. Here we showed that J1R protein in *Cts*45 contains a single P132S mutation. The resulting J1R mutant protein is stable even at the nonpermissive temperature, indicating that the amino acid substitution of residue P132 compromises the function, rather than the stability, of the J1R protein.

We also extended the previous yeast two-hybrid assays to show that recombinant J1R protein forms trimers and that J1R protein self-interacts in virus-infected cells. Based on our domain mapping in two-hybrid analyses, we postulated that the N-terminal region of J1R protein binds to its own C terminus, forming a folded or closed monomeric structure if such an interaction occurs intramolecularly. Alternatively, the N-terminal region of J1R protein could bind to the C terminus of other J1R molecules, resulting in dimers or even oligomers due to head-to-tail intermolecular interactions. At present, our data are consistent with J1R protein forming oligomers through N-to-C intermolecular interactions, although the exact nature of J1R oligomers in virus-infected cells remains to be clarified. Finally, although P132 is situated within the C-terminal self-interaction region, site-directed mutagenesis of the P132 residue generated a P132D mutant that remained self-interactive.

Association of J1R and other viral structural proteins was demonstrated by coimmunoprecipitation of J1R protein with A30L, G7L, and F10L proteins in virus-infected cells. Recently, A30L was shown to be a component of a viral complex

containing G7L and F10L (31, 33). Inclusion of J1R protein in this assembly complex readily explained the identical phenotypes shared by A30L, G7L, and J1R mutant viruses (31, 35). Recently, Szajner et al. described a complex of seven proteins, confirming the interactions of A30L, G7L, F10L, and J1R and also identifying three new interacting proteins, A15L, D2L, and D3R, by mass spectroscopy (30). Furthermore, using confocal microscopy, we showed colocalization of wild-type J1R protein with A30L, G7L, and F10L proteins in virus-infected cells at 24 h p.i. In contrast, a P132D mutant J1R protein was mislocalized, with little colocalization with these three viral proteins in infected cells. Although we do not know whether J1R protein binds directly to A30L, G7L, and F10L proteins or indirectly, through other viral proteins within the complex, our data showed that the P132 residue of J1R protein is critical for formation of a functional complex. In this complex, the role of F10L may be more complicated than those of other component proteins. F10L protein staining in virus-infected cells looked different from that of A30L, G7L, and J1R proteins. Colocalization of J1R protein with F10L kinase was only partial at 24 h p.i. We think that F10L kinase may exist in different viral subcomplexes in cells, and perhaps only some of these F10L-containing complexes have recruited J1R protein. This is consistent with the genetic data showing that F10L kinase is involved in more than one stage of virion morphogenesis and that inactivation of F10L functions has pleiotropic effects on viral membrane formation, IV formation, and A17L processing (19, 32, 33, 37, 41). Besides, Szajner et al. showed that the radioactively labeled protein complexes, when copurified with tagged A30L, A15, or D2 protein, contained much less F10L protein than other components, raising a possibility of subsets of the viral assembly complex existing in cells (30, 33). Further experiments to determine the stoichiometry of each viral protein within the complex will be needed to clarify these differences.

We have previously reported that J1R protein associates with A45R protein in infected cells (6). In this study we showed that J1R protein associated with A30L, G7L, and F10L proteins. Consistent with our data, Szajner's paper showed that J1R protein is present in D2L- and A15L-containing complexes that also contain A30L, G7L, and F10L proteins (30). A45R protein, on the other hand, was not reported in their mass spectrometry analyses. It could be either that the amount of A45R in the A15L-containing complex was too low to be detected or that A45R and J1R proteins form another complex independent of the complex containing A30L, G7L, F10L, D2, and A15L in infected cells. In contrast, our study here revealed that the association of J1R with A30L, G7L, and F10L is important for virion morphogenesis. Furthermore, A45R$^-$ virus still grows well in cell cultures, whereas J1R$^-$ virus is lethal, with a blockage in IV morphogenesis similar to that of A30L$^-$ and G7L$^-$ viruses (1, 6, 31, 35). Thus, A45R protein does not appear to play a functional role in J1R-regulated virion morphogenesis in *Cts*45-infected cells.

Interestingly, J1R protein seemed to regulate the stability of A30L, the 15-kDa form of G7L, and F10L protein in virus-infected cells. The reverse was not true, however; repression of A30L expression did not affect the level of J1R protein in cells (data not shown). We do not yet know whether repression of G7L or F10L protein will affect J1R protein levels in cells. Nevertheless, the role of J1R protein in IV formation involves more than stabilizing A30 protein, since blockage of virus morphogenesis could not be overcome simply by overexpressing A30L protein in the absence of J1R protein (data not shown). Besides, stabilization of G7L protein by J1R protein was specific to the 15-kDa cleavage form of G7L protein, since the stability of the 42-kDa precursor form was not affected by J1R protein levels in cells. Although A30L and the 42-kDa form of G7L protein were previously shown to depend on each other for stability (31, 33), our results showed otherwise, i.e., we detected a stable 42-kDa G7L protein level even when A30L protein was largely degraded in cells infected with viJ1R in the absence of IPTG or with *Cts*45 at 39°C. The reason for this discrepancy is not known and may be related to the threshold of protein degradation in cells. Although unlikely, we cannot totally exclude the possibility that a cross-reacting 42-kDa viral protein comigrates with the 42-kDa form of the G7L protein. Finally, we think that the reduction of F10L protein levels in the absence of J1R protein is an indirect consequence of a reduction of A30L protein levels, since F10L kinase stability is dependent on the A30L and G7L proteins in cells (31, 33).

By immunogold labeling and biochemical extraction experiments, the F10L, A30L, G7L, D2, D3, and A15 proteins appear to be components of the cores (30–33, 35). Although we know that J1R protein is not an integral protein inserted into the microsome membrane fraction (data not shown), the detergent extraction profile indicated that it was present in both membrane and core fractions (6).

In conclusion, in WT VV-infected cells, J1R participates in formation of a protein complex that includes the A30L, G7L, and F10L proteins during IV formation. When J1R is repressed, the integrity of the viral assembly complex is lost and virion morphogenesis is arrested before IV formation, results similar to those found when A30L or G7L was repressed. Finally, the P132 residue is critical for J1R binding to other viral proteins but not for self-interaction. Without association with the J1R protein, other viral components–A30L, G7L (the 15-kDa form), and F10L—become unstable or thermolabile and degrade rapidly.

ACKNOWLEDGMENTS

We thank R. Condit for providing the *Cts*45 mutant virus and Sue-Ping Lee for excellent technical support in electron microscopy.

This work was supported by grants from the Academia Sinica and the National Science Council (NSC93-2320-B-001-006) of the Republic of China.

ADDENDUM

After this work was submitted, another study by Szajner et al. describing a complex of seven vaccinia virus proteins, including J1R protein, was published (30).

REFERENCES

1. **Almazan, F., D. C. Tscharke, and G. L. Smith.** 2001. The vaccinia virus superoxide dismutase-like protein (A45R) is a virion component that is nonessential for virus replication. J. Virol. **75:**7018–7029.
2. **Bartel, P. L., and S. Fields.** 1995. Analyzing protein-protein interactions using two-hybrid system. Methods Enzymol. **254:**241–263.
3. **Betakova, T., E. J. Wolffe, and B. Moss.** 1999. Regulation of vaccinia virus morphogenesis: phosphorylation of the A14L and A17L membrane proteins

and C-terminal truncation of the A17L protein are dependent on the F10L kinase. J. Virol. **73:**3534–3543.
4. **Blasco, R., and B. Moss.** 1991. Extracellular vaccinia virus formation and cell-to-cell virus transmission are prevented by deletion of the gene encoding the 37,000-dalton outer envelope protein. J. Virol. **65:**5910–5920.
5. **Blasco, R., and B. Moss.** 1992. Role of cell-associated enveloped vaccinia virus in cell-to-cell spread. J. Virol. **66:**4170–4179.
6. **Chiu, W. L., and W. Chang.** 2002. Vaccinia virus J1R protein: a viral membrane protein that is essential for virion morphogenesis. J. Virol. **76:**9575–9587.
7. **Condit, R. C., and A. Motyczka.** 1981. Isolation and preliminary characterization of temperature-sensitive mutants of vaccinia virus. Virology **113:**224–241.
8. **Condit, R. C., A. Motyczka, and G. Spizz.** 1983. Isolation, characterization, and physical mapping of temperature-sensitive mutants of vaccinia virus. Virology **128:**429–443.
9. **Dales, S., and L. Siminovitch.** 1961. The development of vaccinia virus in Earles L strain cells as examined by electron microscopy. J. Biophys. Biochem. Cytol. **10:**475–503.
10. **Derrien, M., A. Punjabi, M. Khanna, O. Grubisha, and P. Traktman.** 1999. Tyrosine phosphorylation of A17 during vaccinia virus infection: involvement of the H1 phosphatase and the F10 kinase. J. Virol. **73:**7287–7296.
11. **Geada, M. M., I. Galindo, M. M. Lorenzo, B. Perdiguero, and R. Blasco.** 2001. Movements of vaccinia virus intracellular enveloped virions with GFP tagged to the F13L envelope protein. J. Gen. Virol. **82:**2747–2760.
12. **Grimley, P. M., E. N. Rosenblum, S. J. Mims, and B. Moss.** 1970. Interruption by rifampin of an early stage in vaccinia virus morphogenesis: accumulation of membranes which are precursors of virus envelopes. J. Virol. **6:**519–533.
13. **Hollinshead, M., G. Rodger, H. Van Eijl, M. Law, R. Hollinshead, D. J. Vaux, and G. L. Smith.** 2001. Vaccinia virus utilizes microtubules for movement to the cell surface. J. Cell Biol. **154:**389–402.
14. **Krijnse-Locker, J., S. Schleich, D. Rodriguez, B. Goud, E. J. Snijder, and G. Griffiths.** 1996. The role of a 21-kDa viral membrane protein in the assembly of vaccinia virus from the intermediate compartment. J. Biol. Chem. **271:**14950–14958.
15. **Lackner, C. A., S. M. D'Costa, C. Buck, and R. C. Condit.** 2003. Complementation analysis of the Dales collection of vaccinia virus temperature-sensitive mutants. Virology **305:**240–259.
16. **McCraith, S., T. Holtzman, B. Moss, and S. Fields.** 2000. Genome-wide analysis of vaccinia virus protein-protein interactions. Proc. Natl. Acad. Sci. USA **97:**4879–4884.
17. **Morgan, C., S. Ellison, H. Rose, and D. Moore.** 1954. Structure and development of viruses observed in the electron microscope. II. Vaccinia and fowlpox viruses. J. Exp. Med. **100:**301–310.
18. **Moss, B.** 1996. *Poxviridae*: the viruses and their replication, p. 2637–2671. *In* B. N. Fields, D. M. Knipe, and P. M. Howley (ed.), Fields virology, 3rd ed. Lippincott-Raven Publishers, Philadelphia, Pa.
19. **Punjabi, A., and P. Traktman.** 2005. Cell biological and functional characterization of the vaccinia virus F10 kinase: implications for the mechanism of virion morphogenesis. J. Virol. **79:**2171–2190.
20. **Ravanello, M. P., and D. E. Hruby.** 1994. Characterization of the vaccinia virus L1R myristyl protein as a component of the intracellular virion envelope. J. Gen. Virol. **75:**1479–1483.
21. **Reynolds, E.** 1963. The use of lead citrate at high pH as an electron-opaque stain in electron microscopy. J. Cell Biol. **55:**541–552.
22. **Rietdorf, J., A. Ploubidou, I. Reckmann, A. Holmstrom, F. Frischknecht, M. Zettl, T. Zimmermann, and M. Way.** 2001. Kinesin-dependent movement on microtubules precedes actin-based motility of vaccinia virus. Nat. Cell Biol. **3:**992–1000.
23. **Rodriguez, D., M. Esteban, and J. R. Rodriguez.** 1995. Vaccinia virus A17L gene product is essential for an early step in virion morphogenesis. J. Virol. **69:**4640–4648.
24. **Rodriguez, J. R., C. Risco, J. L. Carrascosa, M. Esteban, and D. Rodriguez.** 1997. Characterization of early stages in vaccinia virus membrane biogenesis: implications of the 21-kilodalton protein and a newly identified 15-kilodalton envelope protein. J. Virol. **71:**1821–1833.
25. **Rodriguez, J. R., C. Risco, J. L. Carrascosa, M. Esteban, and D. Rodriguez.** 1998. Vaccinia virus 15-kilodalton (A14L) protein is essential for assembly and attachment of viral crescents to virosomes. J. Virol. **72:**1287–1296.
26. **Sanderson, C. M., M. Hollinshead, and G. L. Smith.** 2000. The vaccinia virus A27L protein is needed for the microtubule-dependent transport of intracellular mature virus particles. J. Gen. Virol. **81:**47–58.
27. **Sarov, I., and W. K. Joklik.** 1973. Isolation and characterization of intermediates in vaccinia virus morphogenesis. Virology **52:**223–233.
28. **Schmelz, M., B. Sodeik, M. Ericsson, E. J. Wolffe, H. Shida, G. Hiller, and G. Griffiths.** 1994. Assembly of vaccinia virus: the second wrapping cisterna is derived from the *trans*-Golgi network. J. Virol. **68:**130–147.
29. **Spurr, A. R.** 1969. A low-viscosity epoxy resin embedding medium for electron microscopy. J. Ultrastruct. Res. **26:**31–43.
30. **Szajner, P., H. Jaffe, A. S. Weisberg, and B. Moss.** 2004. A complex of seven vaccinia virus proteins conserved in all chordopoxviruses is required for the association of membranes and viroplasm to form immature virions. Virology **330:**447–459.
31. **Szajner, P., H. Jaffe, A. S. Weisberg, and B. Moss.** 2003. Vaccinia virus G7L protein interacts with the A30L protein and is required for association of viral membranes with dense viroplasm to form immature virions. J. Virol. **77:**3418–3429.
32. **Szajner, P., A. S. Weisberg, and B. Moss.** 2004. Evidence for an essential catalytic role of the F10 protein kinase in vaccinia virus morphogenesis. J. Virol. **78:**257–265.
33. **Szajner, P., A. S. Weisberg, and B. Moss.** 2004. Physical and functional interactions between vaccinia virus F10 protein kinase and virion assembly proteins A30 and G7. J. Virol. **78:**266–274.
34. **Szajner, P., A. S. Weisberg, and B. Moss.** 2001. Unique temperature-sensitive defect in vaccinia virus morphogenesis maps to a single nucleotide substitution in the A30L gene. J. Virol. **75:**11222–11226.
35. **Szajner, P., A. S. Weisberg, E. J. Wolffe, and B. Moss.** 2001. Vaccinia virus A30L protein is required for association of viral membranes with dense viroplasm to form immature virions. J. Virol. **75:**5752–5761.
36. **Thompson, C. L., and R. C. Condit.** 1986. Marker rescue mapping of vaccinia virus temperature-sensitive mutants using overlapping cosmid clones representing the entire virus genome. Virology **150:**10–20.
37. **Traktman, P., A. Caligiuri, S. A. Jesty, K. Liu, and U. Sankar.** 1995. Temperature-sensitive mutants with lesions in the vaccinia virus F10 kinase undergo arrest at the earliest stage of virion morphogenesis. J. Virol. **69:**6581–6587.
38. **Traktman, P., K. Liu, J. DeMasi, R. Rollins, S. Jesty, and B. Unger.** 2000. Elucidating the essential role of the A14 phosphoprotein in vaccinia virus morphogenesis: construction and characterization of a tetracycline-inducible recombinant. J. Virol. **74:**3682–3695.
39. **van Eijl, H., M. Hollinshead, G. Rodger, W. H. Zhang, and G. L. Smith.** 2002. The vaccinia virus F12L protein is associated with intracellular enveloped virus particles and is required for their egress to the cell surface. J. Gen. Virol. **83:**195–207.
40. **Vojtek, A. B., and S. M. Hollenberg.** 1995. Ras-Raf interaction: two-hybrid analysis. Methods Enzymol. **255:**331–342.
41. **Wang, S., and S. Shuman.** 1995. Vaccinia virus morphogenesis is blocked by temperature-sensitive mutations in the F10 gene, which encodes protein kinase 2. J. Virol. **69:**6376–6388.
42. **White, C. L., A. S. Weisberg, and B. Moss.** 2000. A glutaredoxin, encoded by the G4L gene of vaccinia virus, is essential for virion morphogenesis. J. Virol. **74:**9175–9183.
43. **Wolffe, E. J., D. M. Moore, P. J. Peters, and B. Moss.** 1996. Vaccinia virus A17L open reading frame encodes an essential component of nascent viral membranes that is required to initiate morphogenesis. J. Virol. **70:**2797–2808.